INTERFACIAL DESIGN FOR DAMAGE TOLERANT FIBER COMPOSITES

V. Damljanovic and N. R. Sottos

Department of Theoretical and Applied Mechanics, University of Illinois at Urbana-Champaign, 104 South Wright Street, Urbana, Illinois 61801, USA

SUMMARY: The study of the interfacial failure during single fiber push-out tests, performed on model polymer composites, reveals the influence of interfacial roughness and adhesion on damage evolution. The experiments showed increasing crack propagation stability, interfacial toughness and frictional stress with increasing roughness. The samples with stronger interfacial adhesion had higher maximum load and interfacial fracture toughness. The occurrence of matrix cracks along the interface was more frequent for rougher fibers as well as for samples with enhanced interfacial adhesion. The push-out force during frictional sliding increased due to various wear mechanisms, whose effects are significant in the case of brittle materials with low surface hardness. These results indicate that the interfacial properties of the model composites can be systematically altered to create a range of damage modes.

KEYWORDS: fiber/matrix interface, push-out, frictional stress, fracture toughness, surface roughness, wear, adhesion.

INTRODUCTION

The structure and properties of the interface in fiber reinforced composites can have a significant effect on the overall mechanical properties of the composite. In particular, the durability characteristics such as strength and fracture toughness are strongly dependent upon the interfacial properties: a strong bond between fiber and matrix facilitates efficient load transfer between the constituents, while a weak interface promotes composite toughness by deflecting cracks into the fiber/matrix interface. Damage accumulation in the region of the interface is responsible for pseudo-ductility in composite materials, which is a key to stress redistribution. Understanding how the interfacial properties are correlated with the damage modes and size of bridging zone, is crucial for designing a composite for a desired application. Various studies of energy dissipation at the interface showed that the toughening contribution from the energy dissipated during frictional sliding of the fiber is much greater than the contribution of the work done during fiber debonding. The difference is more pronounced with the increase in fiber sliding distance. These reflections directed our attention toward identifying the influential interfacial parameters and, in particular, characterizing the frictional sliding after total debond during the single fiber push-out test.

Early theories for the strength and toughness of fiber composites subjected to fiber push-out were based on the simple assumption of constant shear stress at the interface. More recently, Dollar and Steif [1] considered load transfer across an interface which is described by

Coulomb friction. Their theoretical model showed that the constant shear stress approximation overestimates the amount and extent of slip during frictional sliding with the error being more pronounced with increasing friction coefficient and load. The most advanced shear-lag solutions to the fiber push-out problem were developed independently by Liang and Hutchinson [2] and Kerans and Parthasarathy [3], the former being derived by combining the two cases of constant friction and Coulomb friction from model of Hutchinson and Jensen [4]. Nevertheless, these models did not take into account the factors that contribute to the frictional stress, with exception of the model of Kerans and Parthasarathy [3] in which the radial misfit strain due to the surface roughness induces radial stress that contributes to the residual normal stress at the interface. Subsequently, Jero and Kerans [5] provided experimental evidence for the role of asperities using the push-back technique. A characteristic drop in load or "seating drop" allows a distinction to be made between the friction associated with roughness and that due to residual stress at the interface. Jero *et al*. [6] used those experimental observations and the model of Kerans and Parthasarathy [3] to derive the effective interfacial roughness amplitude from the magnitude of the "seating drop".

A more detailed analysis of asperity-controlled friction was reported by Carter *et al*. [7] who calculated the deformation of each asperity from Herzian theory and the axial force exerted by each asperity as a function of a relative displacement. The shear stress they calculated from the axial force, without considering Poisson contraction, had a sinusoidal modulation. From observations on the size and origin of asperities, they concluded that the large asperities, produced by crack deviation during interfacial debonding, and medium-sized asperities, produced during composite fabrication, are the most important contributors to shear load transfer. The smallest asperities, that are result of the fiber production process, are of less importance. The numerical simulations of post-debond frictional sliding by Mackin *et al*. [8] used a model akin to that of Jero *et al*. [6], but with fiber roughness represented by fractal geometry. Using the same solution, Mackin *et al*. [9] confirmed experimental results obtained for a sapphire fiber, with sinusoidal roughness profile, in a glass matrix. They obtained excellent agreement with experimental results for the same fiber in a ceramic matrix by modeling the matrix abrasion with exponential decay in asperity amplitude. Finally, Parthasarathy *et al*. [10] identified a suitable parameter for characterizing the surface roughness effects within the simple elastic mismatch approach used in [3]. They found that the maximum in the coefficients of the Fourier spectrum of the roughness profile, used as an effective roughness amplitude, best correlates the normalized post-peak load with roughness amplitude. However, they also report considerable data scatter and suggest that the model can be used to estimate the effective roughness amplitudes that can be tolerated, or are desirable, in a potential composite.

The common denominator for most of the experimental research on effects of roughness is a focus on fiber and matrix materials with high surface hardness, namely SiC monofilaments in a borosilicate glass matrix [5, 6, 7] or sapphire fibers in TiAl and glass matrices [9]. Due to the high surface hardness, the frictional stress in these systems is expected to have a small contribution from plowing of wear-particles [11, 12]. As noted in [7], the elastic deformation of the asperities is reversible and does not contribute to the over-all strain energy release rate. The porous alumina coatings [9] or weak carbon coatings [6,9] which are used on fibers, act as lubricants and enhance rather than inhibit sliding, since their hardness is much smaller than that of both the fibers and the matrices considered above. Therefore, the neglect of wear in studies mentioned above does not influence the solutions significantly. Nevertheless, Jero *et al*. [6] recognized that wear can be an important mechanism governing the interfacial failure and estimated the effect of abrasion on the magnitude of frictional stress. They compared the

load immediately after debonding (the initial frictional load) with the load immediately before the "seating drop" and explained the decrease in load as an indicator of abrasion.

The model material system used in this study has both fiber and matrix made of polymers, which are generally known for very low surface hardness [11, 12]. Therefore, the wear-particle volume at the interface during frictional sliding and, consequently, the increase in frictional stress, is expected to be considerable. The experimental evidence presented below justifies the expectations and, furthermore, points out the coupling between surface roughness, interfacial adhesion and plowing by wear-particles, which contribute to frictional stress during sliding. Comparisons of our experimental data with existing models which neglect the wear mechanisms, give large errors and reveal the direction for incorporation of adhesion and abrasion into widely used shear-lag models.

EXPERIMENTAL PROCEDURE

Sample preparation

The model composite samples consisted of a single polyester fiber embedded in an epoxy matrix, which were chosen for their birefringent properties. The polyester and epoxy elastic moduli are 3.25 GPa and 4.0 GPa, and Poisson's ratios are 0.35 and 0.33 respectively. A mixture of epoxy resin Epon 828 (diglycidyl ether of bisphenol A) and diethylene-triamine (DETA) curing agent was poured into the mold and over the polyester fiber positioned lengthwise, spanning the opposite walls of the mold. After curing for at least 4 days at room temperature, sample faces parallel to the fiber were polished to 1 μm finish and the bulk sample was cut into 3 to 5 push-out samples of thicknesses varying between 3 and 4.5 fiber diameters. The fiber surface roughness was controlled indirectly by varying the roughness of the rubber molds for polyester fibers. The molds were made by pouring silicon rubber into a master metal mold spanned by 2mm diameter rods made of three different materials: (in order of descending roughness) steel, teflon and glass. After the silicon rubber was cured, the mold for polyester fibers was removed from the metal master mold and the rods were carefully pulled out, leaving channels of various roughnesses. A mixture of general purpose DCPD polyester resin (Superior 61 AA190) and catalyst methyl-ethyl-ketone-peroxide (MEKP-9) was poured into the molds and cured for 48 hours at 40^{o}C. The polyester rods of 1.97 ± 0.03 mm diameter were removed from the mold and their surface roughness profiles were scanned in a Sloan Dektak profilometer. Both average and root-mean-square roughness, ρ_{avg} and ρ_{q} respectively, were recorded. The average roughness was chosen to quantify the fiber surface roughness, since it is considered representative of surface roughness in the related literature [11]. Careful examination of each fiber under the microscope revealed the uniform distribution of asperities and the fiber surface was approximated with a surface generated by revolving the measured roughness profile about the fiber axes. Photographs of representative fibers prior to embedding are given in Fig. 2 (top row). The average fiber surface roughness ρ_{avg}, given in Table 1 varied between 4.3 nm and 153.5 nm.

Table 1: *Ranges of roughnesses of rods for molds and related polyester fibers.*

Rods used to make molds for fibers	ρ_{avg} of polyester fiber [range in nm]	Fiber group
steel	49.5 - 153.5	rough
teflon	15.9 - 33.1	medium
glass	4.3 - 18.6	smooth

The interfacial adhesion was varied by adding coupling agents to the epoxy resin: aminoethyl-aminopropyl-trimethoxysilane (Dow Z-6032) in order to enhance the chemical bonding between epoxy and polyester and dispersion agent methyl-trimetoxysilane (Dow Z-6070) in order to weaken the interface. The polyester rods used for these samples were from the smooth group (Table 2). The samples with coupling agent were polished and cut to the same dimensions as the other samples. Since the interface experiences considerable radial stress due to the chemical shrinkage of epoxy in the process of curing, the residual stress σ_N = -3.32 MPa was indirectly measured using photoelastic fringe multiplication [13] and included in the calculations.

Fiber push-out test

The samples were tested in a push-out apparatus, which was placed in a circular polariscope in order to observe the interfacial failure sequence, following the procedure developed by Bechel and Sottos [13]. In order to minimize bending stresses in the sample, the hole in the steel support was made as small as possible (1.04 fiber diameters), for a punch diameter of 0.85 fiber diameters. The tests were conducted at a punch speed of 5.5 μm/s which was determined to be the upper speed limit at which the loading conditions could still be assumed quasi-static. Force data were collected at a rate of 5 pt/s and corrected in order to account for the load cell drift and the machine compliance of 0.5 μm/N. The fibers were pushed out a distance of 2.75 mm, a little less than half of the fiber length and well past the complete debond so that approximately 4/5 of the data points correspond to frictional sliding. Images of the interfacial failure sequence were acquired by a high-resolution CCD camera (Javelin) and PCI-based IMAQ image acquisition computer board with NI-IMAQ driver software (National Instruments) at the sampling rate of 1 image every 2 seconds. After each test the sample was examined under the microscope and images of the interface and surface of the pushed-out portion of the fiber were recorded.

EXPERIMENTAL RESULTS AND OBSERVATIONS

Surface roughness

Push-out curves for polyester fibers with three different levels of average surface roughness (ρ_{avg}) are shown in Fig.1. Although the initial elastic portions of the push-out curves for samples of different roughnesses were nearly identical, the values of the maximum load and displacement at the onset of sliding were much higher for the rougher fibers. After the initial elastic (linear) part, the push-out curve for the rougher fibers (ρ_{avg} = 62.7nm and 86.4nm) becomes nonlinear which corresponds to progressive debonding. Progressive debonding did not occur in the sample with the smoothest fiber (ρ_{avg} = 6.3nm). The rougher fibers introduce higher stresses at the interface increasing the level of energy needed for crack propagation [3]. Thus, the difference between the energy needed for propagation and that needed for initiation is smaller for rougher samples and the stable crack growth prevails. For smoother fibers, the debond initiation energy is high enough (compared to the debond propagation energy) to cause catastrophic (instantaneous) debonding.

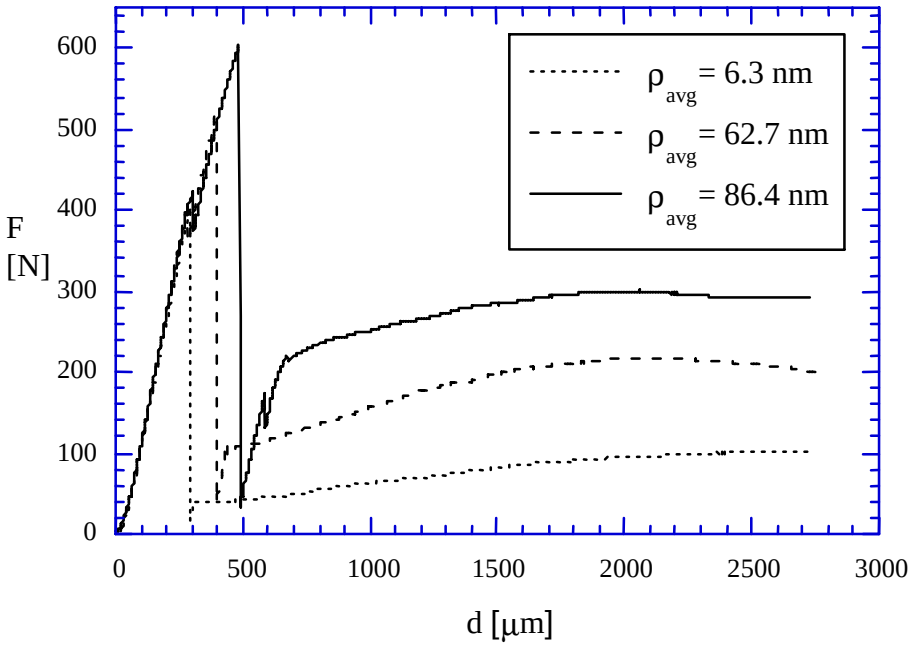

Fig. 1: *Push-out force vs. punch displacement data for samples with different fiber roughnesses.*

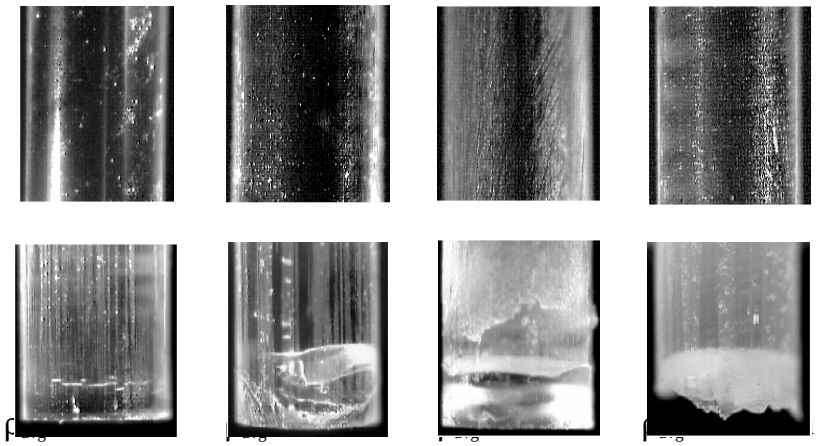

Fig. 2: *Fiber surface before (top) and after (bottom) push-out (12.8 x magnification).*

After complete debonding, the push-out load during frictional sliding increased dramatically with increase in roughness. However, the push-out force is expected to decrease as the fiber pushes out, due to the decrease in contact surface area. Such counterintuitive behavior is due to the strong influence of particle plowing, the evidence of which can clearly be seen on the fiber surfaces after the push-out (Fig. 2, bottom row). The smoothest sample has very fine plowing marks sparsely distributed over the whole surface. The next rougher sample had more and wider plowing marks, which completely covered the surface for the very rough and the roughest sample. The fiber end damage increased for rougher samples and frequently the fiber tip broke off during the debonding for samples of roughnesses larger than 100 nm, due to the high shear stress at the fiber/matrix contact surface.

Interfacial adhesion

The effects of interfacial adhesion were studied on samples with smooth fibers of nearly the same roughness (ρ_{avg} =6-9 nm) with three different levels of adhesion. The addition of Z-6070 dispersion agent significantly reduced the push-out peak load (Fig. 3), while the addition of Z-6032 silane significantly increased the peak load, compared to a sample with no surface treatment. Again, the elastic parts of all three push-out curves were nearly identical. After the initial fluctuations in push-out force immediately after debonding, the force during frictional sliding was nearly the same for all three samples. The slight differences between the push-out curves at the very end of sliding can be explained with the highly random distribution of wear particles between the debonded surfaces. Since all three samples were very smooth, the lack of progressive debonding was not surprising.

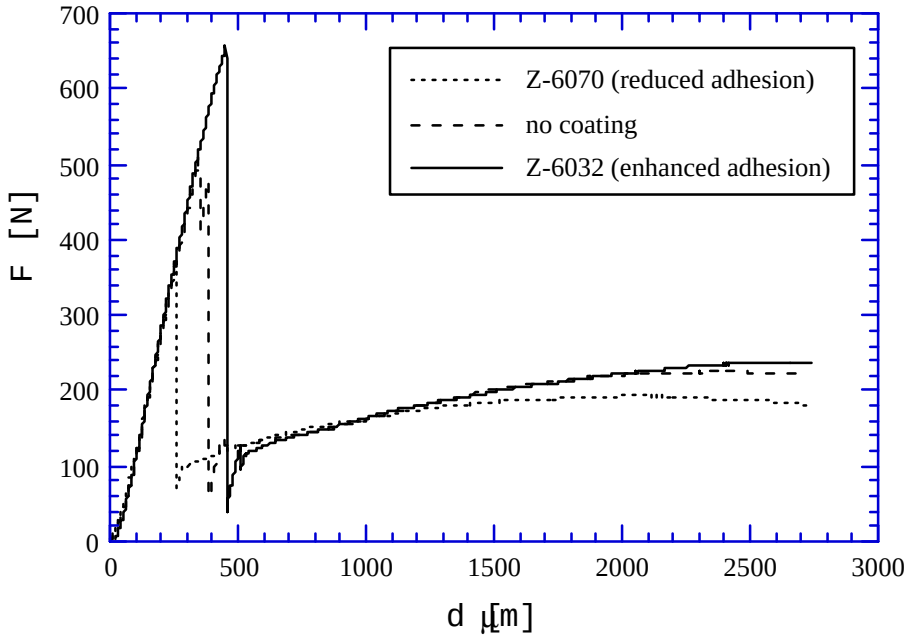

Fig. 3: Push-out force vs punch displacement data for samples with different levels of interfacial adhesion.

During push-out testing, samples with a very strong interface exhibited considerable matrix cracking. In order to further investigate this phenomenon, samples were fabricated with oxidized DETA curing agent and then tested in the push-out apparatus. The curing agent DETA oxidizes with time, which changes the properties of the cured epoxy and enhances the adhesion dramatically. The resulting increase in adhesion is significantly higher than that obtained with Z-6032 silane and leads to very distinct differences in extent of matrix cracking. Samples of medium fiber roughness were cured with four different batches of DETA, aged to a different extent: 0 weeks (Fig. 4a), 12 weeks (Fig. 4b), 16 weeks (Fig. 4c) and 18 weeks (Fig. 4d). Only the sample with unaged DETA had no matrix cracks and the interface experienced plowing as discussed in the previous section. The other three samples had numerous cracks developing away from the interface in planes slightly slanted in the direction of push-out. Due to increased adhesion, the matrix cracks were longer and more frequent for samples with DETA aged longer. The sample with DETA aged the longest (Fig. 4d) also

developed four cracks in vertical planes passing through the fiber axis and the corners of the sample. These vertical cracks started at the top of the sample, from the region of contact between the punch and the fiber and propagated various distances into the material.

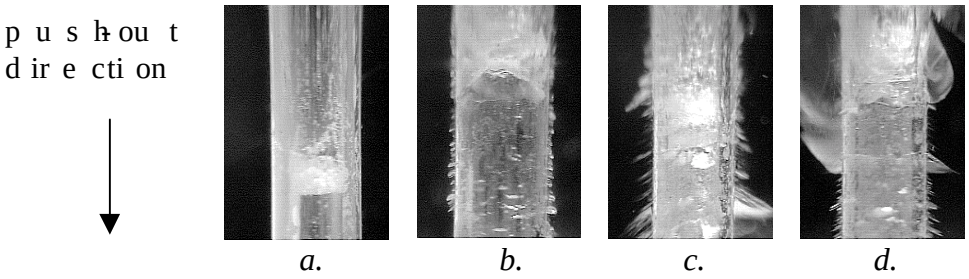

Fig. 4: *Fiber/matrix interface after the push-out: interfacial adhesion is increasing from a. to d. (6.4 x magnification).*

The higher occurrence of matrix cracks indicated increased interface toughness, in agreement with theoretical predictions [14,15]. As the fiber is pushed out, there is a continuing competition between the energy levels needed for crack propagation along the interface and for crack initiation in the matrix. When the crack arrives to the energetically less favorable interface region, it kinks rapidly into the matrix. The shearing of the fiber closes the faces of the matrix crack and it arrests before its length becomes comparable to that of the parent crack, which then continues propagating through the interface again. This process repeats until the fiber is entirely pushed out and more frequently so for the cases of a stronger interface.

FRICTIONAL PROPERTIES DERIVED FROM SHEAR-LAG MODEL

The issue which is important to assessing the push-out data is due to dynamic behavior and involves the stick-slip occurring immediately after the complete debonding and at the onset of frictional sliding. The push-out force fluctuations were more pronounced and the displacement span at which they occur was larger for the rougher samples (Fig. 1). In order to ensure validity of comparisons, the lower displacement limit in the frictional sliding data to be considered was set equal to the displacement at the onset of stable sliding for the roughest sample. The push-out data corresponding to frictional sliding was fit to the shear-lag equation (Eqn. 1a) derived by Kerans and Parthasarathy [3],

$$d = t - \frac{1}{C_3 \mu} \ln\left(1 - \frac{F}{P^*}\right) \tag{1a}$$

$$F = \left(C_1\sqrt{G_{IIc}} + P_r - P^*\right) e^{C_3 \mu L_d} \tag{1b}$$

where d is the punch displacement, t is the fiber length, C_3 is equal to fiber radius divided by material constant, μ is coefficient of friction, F is a push-out force and P^* is the critical axial load necessary to open the interface in the pull-out. The coefficients of friction were 0.456, 0.653 and 0.746 for fiber roughness of 6.3nm, 62.7nm and 86.4nm respectively. As seen in

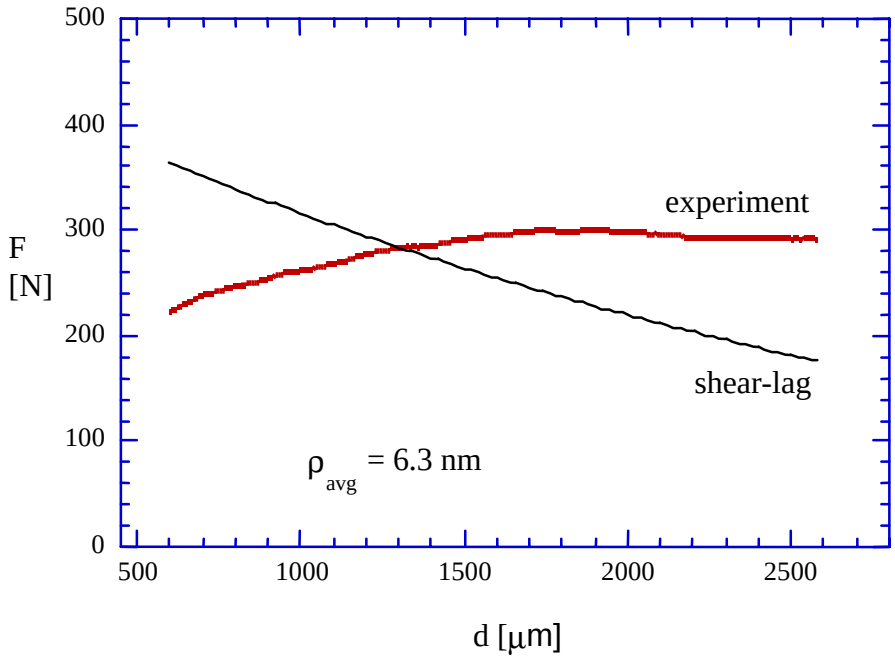

Fig.5: *Comparison of experimental data and shear-lag prediction of frictional sliding for the smoothest fiber.*

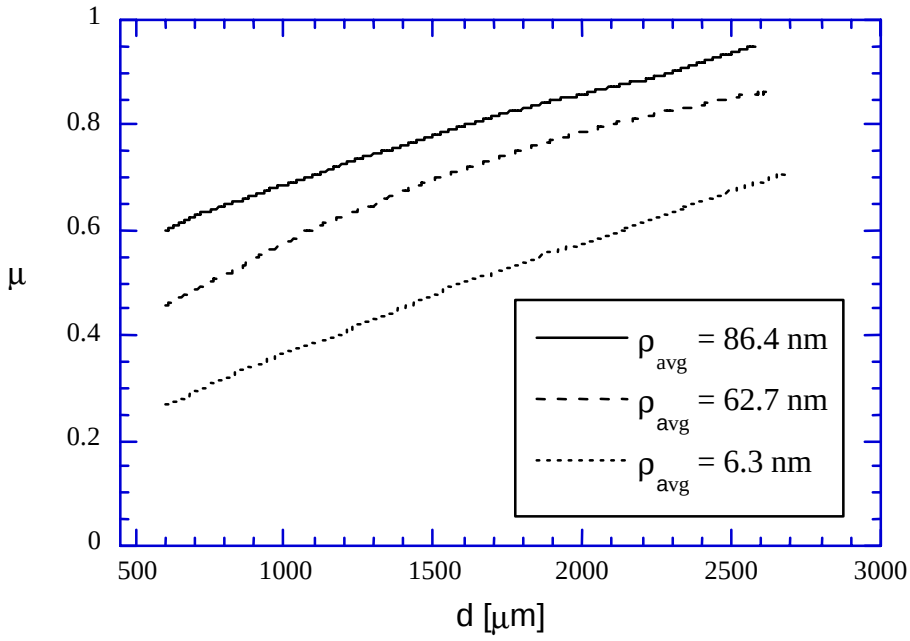

Fig. 6: *Point-wise calculation of μ from shear-lag solution.*

Fig. 5, the error of these curve-fits was significant, even for the smooth fiber, due to wear mechanisms were not accounted for in the model. The coefficient of friction calculated point-wise from experimental data and plotted versus punch displacement, increased during push-out (Fig. 6). Even though the same shear-lag model was employed in these calculations, it is clear that the coefficient of friction cannot be considered a material constant but rather a property influenced by both surface morphology and wear mechanisms. These difficulties

also affect the calculations of mode II fracture toughness, G_{IIc}, from the Eqn. 1b which corresponds to the progressive debonding. In the case of brittle material systems with low surface hardness, a meaningful value of fracture toughness can not be calculated from shear-lag since it relies on the inaccurate value of coefficient of friction. The fracture toughness obtained in such way is too high for this material system and cannot be used as a valid interface characteristic. These conclusion brings forward the theory of friction space postulated by Suh and Sin [16], as the modification which can be incorporated into the shear-lag model. The friction coefficient is represented in the friction space as a sum of contributions due to the deformation of surface asperities, plowing by wear particles and adhesion of the flat contact. The implementation of this model will be further investigated in order to obtain a more detailed model of frictional sliding.

CONCLUSIONS

Our experimental results from the push-out tests performed on the model composites, indicate that systematic altering of interfacial roughness and adhesion can be used to create a range of damage modes. However, the experimental push-out curves cannot be predicted accurately by shear-lag solution, due to the fact that it does not take into account the wear mechanisms at the debonded interface. These mechanisms can be neglected in cases of high surface hardness and/or weak or porous fiber coatings, but are crucial in the case of brittle material systems with both surfaces of low hardness. In order to account for wear, the coefficient of friction in shear-lag model should be modified to include effects of adhesion, roughness and plowing by wear particles.

ACKNOWLEDGEMENTS

This work was completed with support from the U.S.A. Air Force Office of Scientific Research under Grant F49620-98-1-0084. The profilometric study was carried out by Tom Berfield in the Center for Microanalysis of Materials, University of Illinois, which is supported by the U.S. Department of Energy under Grant DEFG02-91-ER45439. The first author would like to thank Pranav Shrotriya for helping in residual stress calculation. The authors would also like to acknowledge the insight of Dr. V. Bechel from the Wright Patterson Laboratory and Professor T. Mackin from the University of Illinois.

REFERENCES

1. Dollar, A. and Steif, P.S., "Load Transfer in Composites With a Coulomb Friction Interface", *International Journal of Solids Structures*, Vol. 24, No.8, 1988, pp. 789-803.

2. Liang, C. and Hutchinson, J.W., “Mechanics of the Fiber Pushout Test”, *Mechanics of Materials*, Vol. 14, 1993, pp. 207-221.

3. Kerans, R.J. and Parthasarathy, T.A., "Theoretical Analysis of the Fiber Pullout and Pushout Tests", *Journal of American Ceramic Society*, Vol. 74, No.7, 1991, pp. 1585-1596.

4. Hutchinson, J.W. and Jensen, H.M, "Models of Fiber Debonding and Pullout in Brittle Composites With Friction", *Mechanics of Materials*, Vol. 9, 1990, pp. 139-163.

5. Jero, P.D. and Kerans, R.J., "The Contribution of Interfacial Roughness to Sliding Friction of Ceramic Fibers in a Glass Matrix", *Scripta Metallurgica et Materialia*, Vol. 24, 1990, pp. 2315-2318.

6. Jero, P.D., Kerans, R.J. and Parthasarathy, T.A., "Effect of Interfacial Roughness on the Frictional Stress Measured Using Pushout Tests", *Journal of American Ceramic Society*, Vol. 74, No.11, 1991, pp. 2793-2801.

7. Carter, W.C., Butler, E.P. and Fuller, E.R. , "Micro-Mechanical Aspects of Asperity-Controlled Friction in Fiber-Toughened Ceramic Composites", Scripta Metallurgica et Materialia, Vol.25, 1991, pp. 579-584.

8. Mackin, T.J., Warren, P.D. and Evans, A.G., " Effects of Fiber Roughness on Interface Sliding in Composites", *Acta Metallica et Materialia*, Vol. 40, No.6, 1992, pp. 1251-1257.

9. Mackin, T.J., Yang, J. and Warren, P.D., " Influence of Fiber Roughness on the Sliding Behavior of Sapphire Fibers in TiAl and Glass Matrices", *Journal of American Ceramic Society*, Vol. 75, No.12, 1992, pp. 3358-3362.

10. Parthasarathy, T.A., Barlage, D.R., Jero, P.D. and Kerans, R.J., "Effect of Interfacial Roughness Parameters on the Fiber Pushout Behavior of a Model Composite", *Journal of American Ceramic Society*, Vol. 77, No.12, 1994, pp. 3232-3236.

11. Suh, N.P., *Tribophysics*, Prentice-Hall Inc., Englewood Cliffs, New Jersey, 1986.

12. Yamaguchi, Y., *Tribology of Plastic Materials*, Elsevier, New York, 1990.

13. Bechel, V.T. and Sottos, N.R., “Application of Debond Length Measurements to Examine the Mechanics of Fiber Pushout”, *Journal of Mechanics and Physics of Solids*,Vol.46, No.9, 1998, pp. 1675-1697.

14. He, M. and Hutchinson, J.W., "Kinking of a Crack Out of an Interface", *Journal of Applied Mechanics*, Transactions of the ASME, Vol. 56, June 1989, pp. 270-278.

15. Dollar, A. and Steif, P.S., " Interface Blunting of Matrix Cracks in Fiber- Reinforced Ceramics", *Journal of Applied Mechanics*, Transactions of the ASME, Vol. 59, December 1992, pp. 796-803.

16. Suh, N.P. and Sin, H.C., "The Genesis of Friction", *Wear*, Vol. 69, 1981, pp. 91-114.